RESEARCH ARTICLE

Bacterial Cell Enlargement Requires Control of Cell Wall Stiffness Mediated by Peptidoglycan Hydrolases

Richard Wheeler,* Robert D. Turner, Richard G. Bailey, Bartłomiej Salamaga, Stéphane Mesnage, Sharifah A. S. Mohamad,* Emma J. Hayhurst,* Malcolm Horsburgh,* Jamie K. Hobbs, Simon J. Foster

Krebs Institute, University of Sheffield, Firth Court, Western Bank, Sheffield, United Kingdom

* Present address: Richard Wheeler, Biology and Genetics of the Bacterial Cell Wall Unit, Institut Pasteur, and INSERM, Avenir group, Paris, France; Sharifah A. S. Mohamad, Faculty of Applied Sciences, Universiti Teknologi MARA, Shah Alam, Selangor, Selangor, Malaysia; Emma J. Hayhurst, Faculty of Computing, Engineering and Science, University of South Wales, Pontypridd, United Kingdom; Malcolm Horsburgh, Institute of Integrative Biology, Biosciences Building, University of Liverpool, Crown Street, Liverpool, United Kingdom.

R.W. and R.D.T are joint first authors who contributed equally to this work.

ABSTRACT **Most bacterial cells are enclosed in a single macromolecule of the cell wall polymer, peptidoglycan, which is required for shape determination and maintenance of viability, while peptidoglycan biosynthesis is an important antibiotic target. It is hypothesized that cellular enlargement requires regional expansion of the cell wall through coordinated insertion and hydrolysis of peptidoglycan. Here, a group of (apparent glucosaminidase) peptidoglycan hydrolases are identified that are together required for cell enlargement and correct cellular morphology of *Staphylococcus aureus*, demonstrating the overall importance of this enzyme activity. These are Atl, SagA, ScaH, and SagB. The major advance here is the explanation of the observed morphological defects in terms of the mechanical and biochemical properties of peptidoglycan. It was shown that cells lacking groups of these hydrolases have increased surface stiffness and, in the absence of SagB, substantially increased glycan chain length. This indicates that, beyond their established roles (for example in cell separation), some hydrolases enable cellular enlargement by making peptidoglycan easier to stretch, providing the first direct evidence demonstrating that cellular enlargement occurs via modulation of the mechanical properties of peptidoglycan.**

IMPORTANCE **Understanding bacterial growth and division is a fundamental problem, and knowledge in this area underlies the treatment of many infectious diseases. Almost all bacteria are surrounded by a macromolecule of peptidoglycan that encloses the cell and maintains shape, and bacterial cells must increase the size of this molecule in order to enlarge themselves. This requires not only the insertion of new peptidoglycan monomers, a process targeted by antibiotics, including penicillin, but also breakage of existing bonds, a potentially hazardous activity for the cell. Using *Staphylococcus aureus*, we have identified a set of enzymes that are critical for cellular enlargement. We show that these enzymes are required for normal growth and define the mechanism through which cellular enlargement is accomplished, i.e., by breaking bonds in the peptidoglycan, which reduces the stiffness of the cell wall, enabling it to stretch and expand, a process that is likely to be fundamental to many bacteria.**

Received 24 April 2015 **Accepted** 11 June 2015 **Published** 28 July 2015

Citation Wheeler R, Turner RD, Bailey RG, Salamaga B, Mesnage S, Mohamad SAS, Hayhurst EJ, Horsburgh M, Hobbs JK, Foster SJ. 2015. Bacterial cell enlargement requires control of cell wall stiffness mediated by peptidoglycan hydrolases. mBio 6(4):e00660-15. doi:10.1128/mBio.00660-15.

Editor Arturo Casadevall, Johns Hopkins Bloomberg School of Public Health

Address correspondence to Simon J. Foster, s.foster@sheffield.ac.uk.

In almost all bacteria, the major stress-bearing component of the cell envelope is a single, polymeric macromolecule of peptidoglycan. In order for an individual cell to grow (enlarge), new monomeric precursors are added to the peptidoglycan sacculus. These are inserted by penicillin binding proteins (PBPs), guided by a complex machinery involving many components (1). However, enlargement of the sacculus cannot occur solely through the addition of new material. Existing bonds must be cut in order that the sacculus can permanently expand via accommodation of more material. This activity is executed by peptidoglycan hydrolases. These break specific amide and glycosidic bonds in the sacculus, prompting the idea that some of these enzymes are required for the enlargement of individual bacterial cells and, consequently, for bacterial population growth.

While there is likely to be great variation in cellular enlargement mechanisms across the array of bacterial species, there is a broadly held assumption that new peptidoglycan monomers are inserted such that they do not initially experience stress derived from turgor pressure. The idea is that stress is subsequently placed on this new material due to the breaking of bonds within older peptidoglycan, allowing the sacculus as a whole to expand. While completely reasonable and therefore widely accepted, this assumption is largely unsupported by experimental evidence. This concept underpins the two major models of cellular enlargement, one of which is for elongation of rod-shaped Gram-positive species and the other for *Escherichia coli*. In rod-shaped Gram-positive bacteria, "inside-to-outside growth" is proposed (2). New monomers are applied at a high surface density close to the inner

surface of the cell wall (the only region accessible to the membrane-bound PBPs). As subsequent layers are added, the older material is enzymatically degraded, causing stress to be applied to the new material and the sacculus to expand. In *E. coli*, the "three for one" model states that three new peptidoglycan monomers are added in a loop around an existing monomer (3). When the bonds attaching the existing monomer to its neighbors are broken, stress is applied to the new loop, enabling expansion of the sacculus. While they differ in detail, both of these models invoke breaking of bonds within peptidoglycan and, thus, hydrolase activity.

The necessity of hydrolases in cellular enlargement models suggests that removing hydrolase activity should arrest this process, causing the cell to stop dividing and ultimately terminating the growth of the population, but surprisingly, there is only one example of a hydrolase-encoding gene that is individually essential for survival, *pcsB* in *Streptococcus pneumoniae* (4, 5). However, there are groups of hydrolases that are synthetically essential. In *Bacillus subtilis*, removal of YvcE (CwlO) and LytE terminates cell elongation and, thus, population growth (6), and in *E. coli*, loss of Spr, YdhO, and YebA leads to an increasingly ellipsoid cell shape and synthetic lethality (7). The existence of individually or collectively essential hydrolases in these diverse species strongly suggests a general phenomenon applicable to many other bacteria: that bacterial cellular enlargement and thus, ultimately, division and population growth depend on the ability of cells to hydrolyze peptidoglycan (8). However, the detailed mechanisms by which hydrolysis enables individual cells to enlarge remain unclear.

In many species of bacteria, including *E. coli*, *B. subtilis*, and *S. pneumoniae*, cellular enlargement is accomplished by two machineries (groups of proteins that work together to execute a cellular process), one for elongation and another for division (9). In these species, hydrolases can potentially be attributed separately to either of these machineries (10). *Staphylococcus aureus* presents a simplified system in which to study the role of hydrolases in cell enlargement, as it is roughly spherical and does not have a specific elongation machinery. Insertion of peptidoglycan apparently occurs only during septation (11, 12), while cell volume increases at a constant rate throughout the cell cycle (13), before the process is repeated on a plane orthogonal to the two previous divisions (14). The septal disc is initially protected from the level of turgor-induced stress experienced by the rest of the cell wall, as it is formed inside the cell. For this reason and the absence of a preexisting layer of cell wall at the beginning of septation, the inside-to-outside-growth model cannot be applied. Maturation of the septal disc is accompanied by alterations in peptidoglycan architecture and mechanical properties. The nanoscale surface architecture of the peptidoglycan changes from a ring like (15) to a knobbly (punctate) pattern (11). This is accompanied by changes in the stiffness of the cell surface; Atomic Force Microscopy (AFM) has shown that recently revealed septal cell wall is stiffer than mature cell wall (16).

S. aureus has numerous genes encoding peptidoglycan hydrolases (17–19). Here, we focus on *N*-acetylglucosaminidases (glucosaminidases), a class of cell wall hydrolases that target the bond between the *N*-acetylglucosamine and *N*-acetylmuramic acid residues in the polysaccharide (glycan) backbone of peptidoglycan. *S. aureus* has very short glycan strands compared to many other Gram-positive species, attributed to prolific glucosaminidase activity (20, 21). Previously, the only glucosaminidase characterized in *S. aureus* was the bifunctional glucosaminidase *N*-acetylmuramyl-L-alanine amidase, Atl, thought to be primarily involved in cell division (22, 23).

In this study, we report that a previously uncharacterized enzyme, SagB, is the major glucosaminidase for processing of glycan chains in *S. aureus*. We unravel the mechanisms connecting the biochemical activity of glucosaminidases to the mechanical properties of the cell wall, the cellular morphology and, ultimately, the capacity of the bacterial cells to enlarge and the population to grow. We propose that, as previously speculated, modulation of cell wall mechanical properties by hydrolases is a general mechanism for the enlargement of bacterial cells, with the timing and synchronicity of insertion and hydrolysis differing widely between species.

RESULTS

Shape changes and cell wall alteration throughout the cell cycle. Cellular morphological dynamics were investigated using fluorescence microscopy of living cells stained with FM 1-43 to visualize the membrane. Of 100 cell cycle events scrutinized in detail, all cells exhibited a rapid splitting event within the 15-s interval between camera frames (Fig. 1a). This is consistent with very recently published data showing that this process occurs within milliseconds and that cell volume increase occurs at a constant rate throughout the cell cycle, leading to a prolate morphology (13). The splitting is preceded by the cell surface scission event previously observed during AFM imaging of cell division (24, 25).

AFM imaging (11) and force measurements (16) indicate that septal peptidoglycan changes as it matures. To investigate this further, the accessibility of peptidoglycan to a large peptidoglycan-binding probe was assessed in *S. aureus* wild-type strain SH1000 cells (Fig. 1b). Wheat Germ Agglutinin-Alexa Fluor 350 conjugate (WGA-AF350; heterodimer of approximately 38 kDa) is a GlcNAc-binding lectin. Although the GlcNAc-MurNAc glycan motif is ubiquitous, in many instances, the WGA-AF350 complex labeled only part of the cell. Comparison with fluorescent vancomycin (Van-FL) labeling, which binds the pentapeptide that is prevalent in regions of newly inserted peptidoglycan and is thus a marker of nascent cell wall (26), revealed that WGA-AF350 preferentially bound the mature cell wall but was excluded from the septum. This suggests that the architecture of the nascent cell wall hinders access by the large WGA lectin, whereas in matured cells, the peptidoglycan is labeled homogenously. In contrast, the approximately 22-fold-smaller Van-FL (~1.5 kDa) could access the nascent peptidoglycan, even when daughter cells were not separated, further evidence of modification of the peptidoglycan network.

Glucosaminidases are critical for population growth in *S. aureus*. Given that the short glycan chain length in *S. aureus* suggests a major role for glucosaminidases in overall peptidoglycan hydrolysis, we hypothesized that inactivation of all glucosaminidase activity would have an impact on population growth. Four enzymes with glucosaminidase activity (known and putative) were identified by BLAST searches against the known glucosaminidase domain of Atl (Fig. 2a; see also Fig. S1 in the supplemental material). Those identified are *atl* (23) and three additional glucosaminidase domain-encoding genes, for which the nomenclature *sagA* (SACOL2298) and *sagB* (SACOL1825), for *S. aureus* glucosaminidase A and B, respectively, and *scaH* (SACOL2666) is proposed. Gene inactivations were made in each of the four, and every combination of triple mutant con-

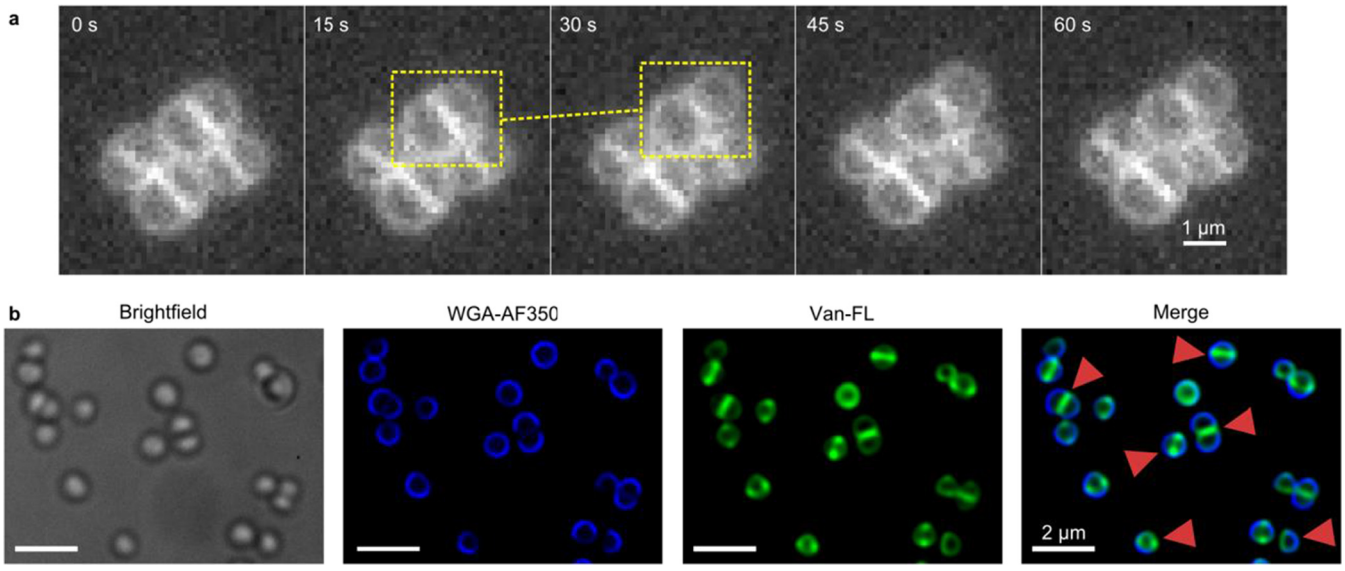

FIG 1 Morphological dynamics during the cell cycle of *S. aureus*. (a) FM 1-43 labeling of living *S. aureus* SH1000 cells shows that the bacteria change shape rapidly immediately after division (see dashed boxes). (b) Images of *S. aureus* after labeling of the cell wall with Van-FL (~1.7-kDa) and WGA-AF350 (~38-kDa) fluorescent probe molecules. Arrowheads show cells where Van-FL is bound to regions from which WGA-AF350 has been excluded.

structed in *S. aureus* SH1000 (Table 1, Table 2, and Table 3). Despite repeated attempts, we were unable to obtain a strain in which all four putative glucosaminidase-encoding genes were inactivated, prompting the hypothesis that glucosaminidase activity is essential. To test this, a conditional quadruple glucosaminidase mutant was constructed by inserting an inducible *sagB* expression construct into the SH4611 (*atl sagA scaH*) triple mutant background. The resulting strain, SH4615 (P_{spac}-*sagB atl sagA scaH*), contains a truncated copy of *sagB* under the control of the native promoter and a full copy of *sagB* under the isopropyl-β-D-thiogalactopyranoside (IPTG)-inducible P_{spac} promoter (see Fig. S2 in the supplemental material).

The importance of glucosaminidase activity was assessed by plating the conditional mutant on solid medium in the presence of 1 mM IPTG and then streaking single colonies onto solid medium with or without IPTG (Fig. 2b). In the absence of IPTG, little growth was observed. Thus, it is not the individual enzymes that are required, as they are functionally redundant, but more likely glucosaminidase activity itself.

Although inactivation of *sagB* alone did not affect growth on solid medium (data not shown), in liquid medium, inactivation of *sagB* alone led to a substantial increase in doubling time [for SH1000, 30 ± 1 min (mean ± standard error), and for SH4608 (*sagB*), 43 ± 2 min] and yield (see Fig. S3 in the supplemental material). Strain SH4615 (P_{spac}-*sagB atl sagA scaH*) without IPTG exhibited a longer doubling time (50 ± 4 min) than SH4608 (*sagB*), SH4611 (*atl sagA scaH*), and SH4615 (P_{spac}-*sagB atl sagA scaH*) with IPTG.

Cells lacking glucosaminidases have morphological defects. Exponential-phase cells (optical density at 600 nm [OD_{600}] of

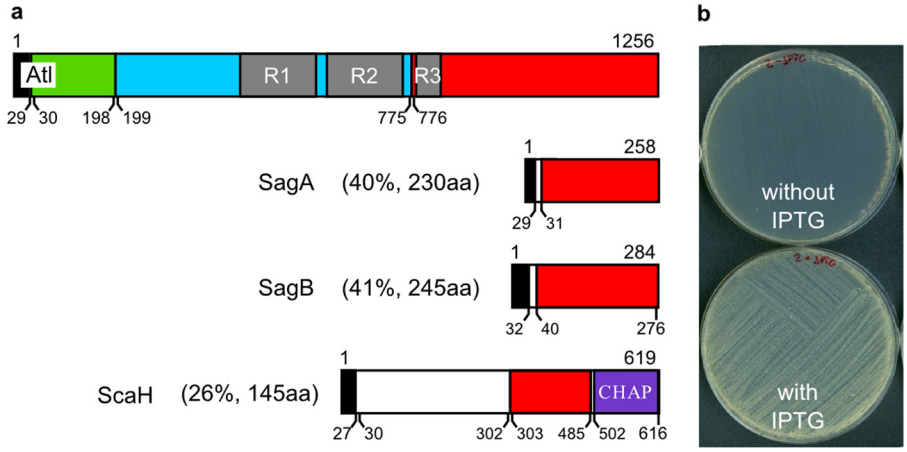

FIG 2 Role of glucosaminidases in population growth. (a) Physical map showing the domain structure of putative glucosaminidases of *S. aureus*. Percentage homology to Atl glucosaminidase domain and length of homologous amino acid sequence (aa) are indicated in brackets. Black, signal peptide; green, propeptide; grey, repeat domains R1, R2, and R3; blue, *N*-acetyl-muramyl-L-alanine amidase domain; red, *N*-acetyl-β-D-glucosaminidase domain; purple, cysteine, histidine-dependent amidohydrolase/peptidase (CHAP) domain. (b) Growth of SH4615 (P_{spac}-*sagB atl sagA scaH*) with or without IPTG.

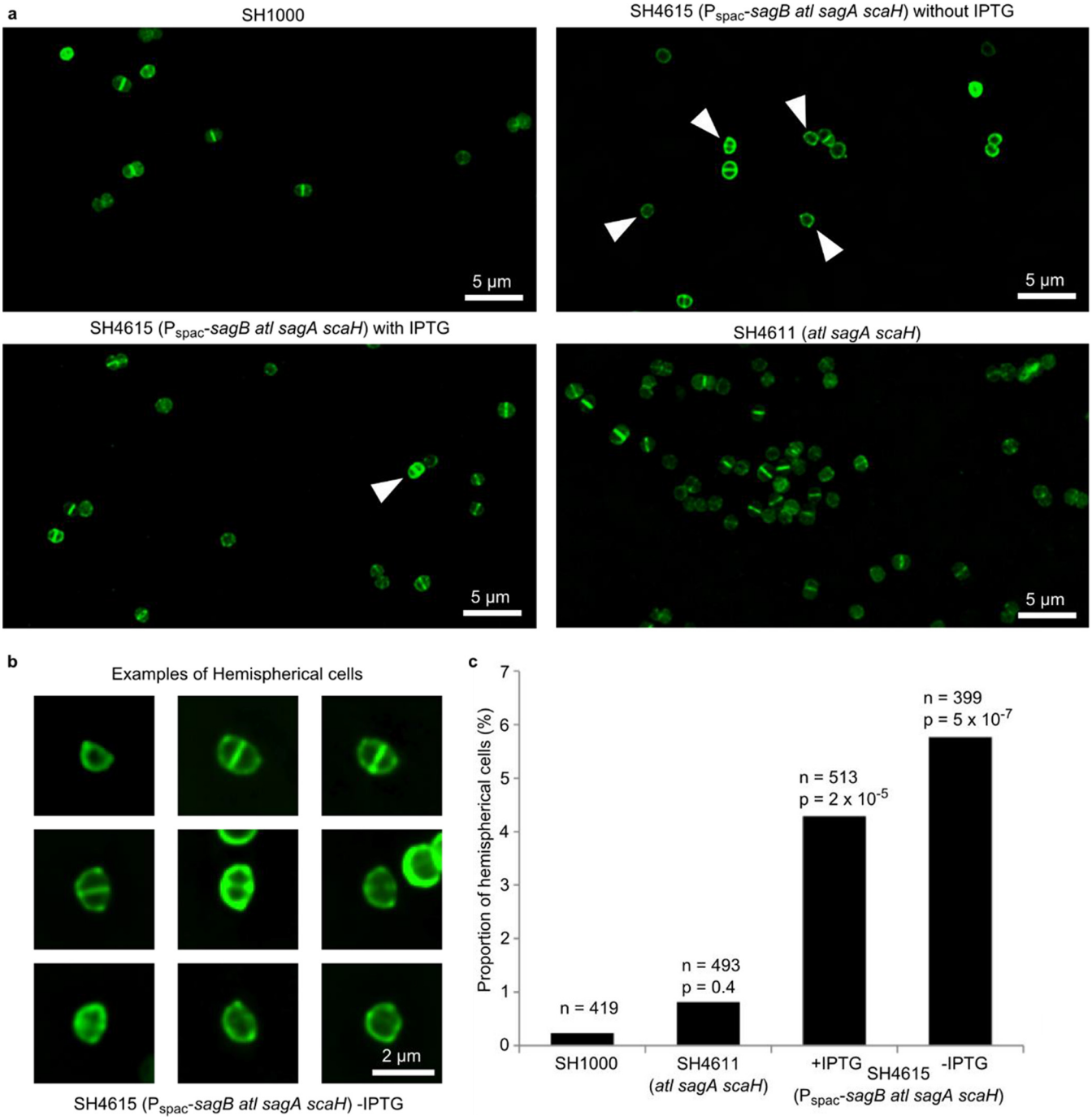

FIG 3 Morphological defects in *S. aureus* cells lacking glucosaminidases. (a) Images of fixed, Van-FL-labeled cells showing altered morphology. Arrowheads indicate hemispherical cells. Cells of this shape are not found in wild-type populations unless attached to a sister cell. (b) Examples of hemispherical cells. In some cells, septa are visible in bacteria that have not completed the shape change to the mature spherical morphology. This shows that correct shape change is not taking place within the duration of the cell cycle. (c) Quantification of the proportion of hemispherical cells in each sample. *P* values are the result of Fisher's exact tests comparing the wild type with each mutant.

~0.3) were labeled with Van-FL prior to fixation, to visualize the cell wall and plane of septation. In wild-type SH1000, the normal range of roughly spherical-to-prolate shapes with or without septa were identified (11). However, in SH4615 (P_{spac}-*sagB atl sagA scaH*) without IPTG, roughly hemispherical cells distinct from previously observed wild-type morphologies were observed (Fig. 3a and b). These hemispherical cells were not attached to their sisters, and in some cases, these were bisected by a nascent septum despite not yet having expanded into the mature morphology. This shows that normal cellular enlargement has failed to take place prior to the cell attempting to initiate another round of division. Hemispherical cells were also observed at lower preva-

lence in SH4615 (P_{spac}-*sagB atl sagA scaH*) with IPTG and in SH4611 (*atl sagA scaH*) (Fig. 3c), suggesting that expression from the P_{spac} promoter is insufficient to give native levels of SagB. In SH4608 (*sagB*), very few hemispherical cells were observed (see Fig. S4 in the supplemental material). To summarize, cells impaired in glucosaminidase activity are also impaired in their ability to increase in size after division and adopt the correct mature shape.

SagB modulates cell wall elasticity. In order to investigate the relationship between the ability of cells to enlarge and assume correct morphology and cell wall mechanical properties, the stiffness of the cell wall was measured using AFM in several glucosaminidase mutants. This enabled exploration of the possibility that increased stiffness (i.e., more force must be applied to result in the same amount of stretching of the cell wall) is associated with impaired glucosaminidase activity (Fig. 4). With this approach, a force is applied by an AFM tip to a surface of interest and the resulting deflection of the cantilever and, thus, indentation of the cell surface is measured. By measuring the gradient of a tangent to this force-displacement curve in the region of low deformation, a relative measure of cell surface stiffness is obtained independently of overall cell deformation and turgor. More sophisticated contact mechanics models were not employed for reasons described previously (16). The measurements were taken from multiple points on the surface of the cell (Fig. 4a) in regions not specifically identified as recently having been part of the septal plate, i.e., regions lacking ring or spiral surface architecture.

In strains lacking any combination of three glucosaminidase-encoding genes, the median cell wall stiffness was significantly increased (Wilcoxon rank sum test) compared with that of the wild-type strain SH1000 (Fig. 4b; also see Table S1 in the supplemental material). In all strains combining other mutations with *sagB*, the cell wall stiffness was similar to that of SH4608 (*sagB*) cells. SH4611 (*atl sagA scaH*) cells had cell walls that were stiffer than those of SH1000 cells but less stiff than the cell walls of any strain lacking *sagB*. Chromosomal complementation of the *sagB* deletion using the native promoter led to almost complete restoration of wild-type stiffness. Thus, even though SagB has the most profound role in cell wall stiffness determination, there is an important contribution from the other three enzymes.

SagB regulates glycan chain length. The bulk properties of a polymer (such as peptidoglycan) are a consequence of its nanoscale structure. Glucosaminidases might therefore modify the mechanical properties of peptidoglycan, making it less stiff, through reduction of glycan strand length. In order to establish whether the observed stiffness changes could be ascribed to altered chain length, we investigated the individual contribution of each glucosaminidase to glycan chain length regulation, using size exclusion chromatography to analyze the chain length of purified *N*-acetyl[^{14}C]glucosamine ([^{14}C]GlcNAc)-labeled glycans (Fig. 5; see also Fig. S5 and S6 in the supplemental material).

Consistent with previously published data (20, 21), wild-type *S. aureus* had predominantly short glycan chains (on average, 6 to 10 dissacharides), with approximately 30% of glycan chains exceeding 50 dissacharides in length (Fig. 5; see also Fig. S5 and S6 in the supplemental material). However, inactivation of *sagB* resulted in a substantial increase in the proportion of long glycan strands (52.5% had >50 disaccharides). Complementation of

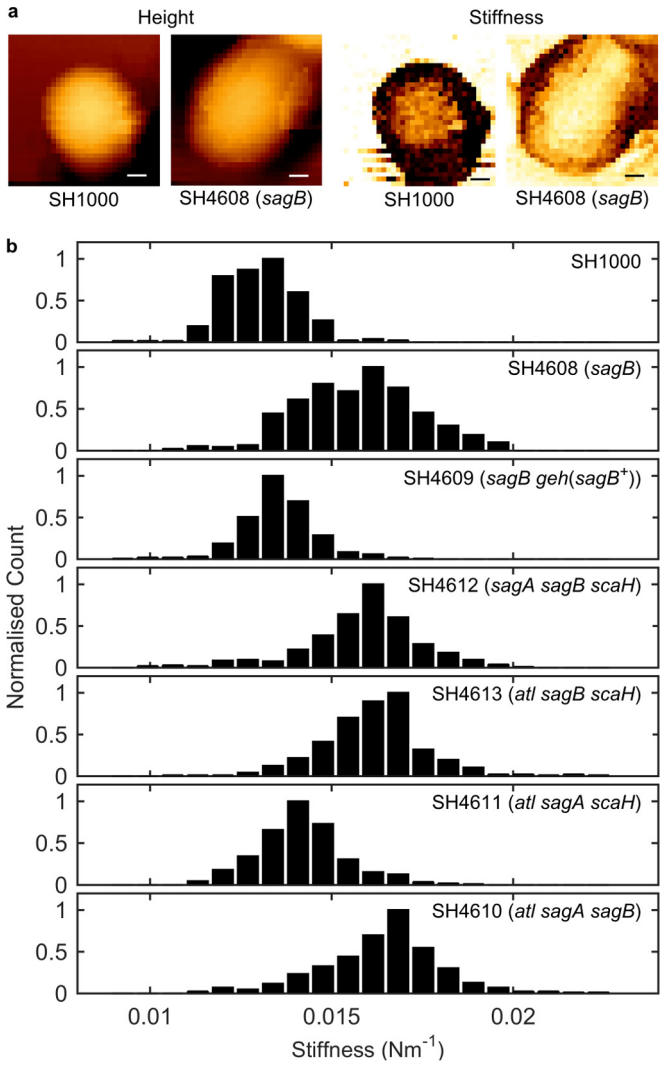

FIG 4 Mechanical properties of the *S. aureus* cell wall. (a) AFM heights and effective spring constants (stiffness maps) of SH1000 and SH4608 (*sagB*) derived from force maps. In the height map, regions with a lighter color are higher than darker regions. In the stiffness map, regions with a lighter color are stiffer than darker regions. Scale bars, 200 nm; height scale, 500 nm; stiffness scale, 0.010 to 0.018 Nm^{-1}. (b) Stiffness of the cell wall of wild-type and glucosaminidase mutant strains, derived from AFM force maps.

sagB restored the wild-type chain length distribution (32.9% had >50 disaccharides) (Fig. 5).

Of the strains lacking three glucosaminidases, cells of all strains carrying the *sagB* inactivation had an increased proportion of long glycan strands (48.4 to 59.3% had >50 disaccharides) (Fig. 5). In these cases, the proportion was even higher than for SH4608 (*sagB*). Strains with inactivations in both *sagA* and *sagB* have the highest proportion of long glycans. This suggests a modest additional impact on chain length from Atl, ScaH, and in particular, SagA. SH4611 (*atl sagA scaH*), in which SagB was the sole remaining glucosaminidase, had a glycan chain length distribution similar to that of SH1000 (32.5% had >50 disaccharides). Thus, SagB has a dominant enzymatic activity and is the major glucosaminidase responsible for the archetypical short glycan chain length of *S. aureus*. Furthermore, this activity is nonredundant, as the pres-

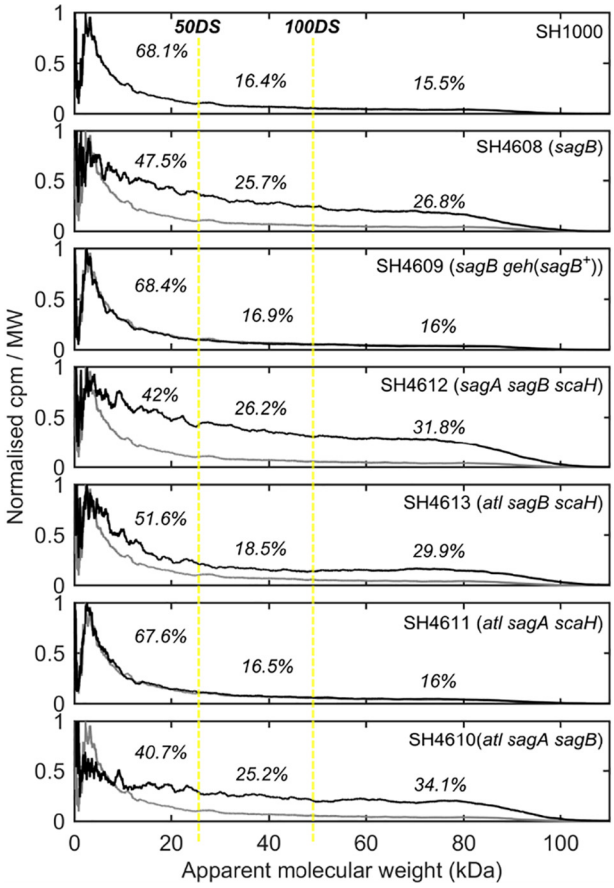

FIG 5 Role of glucosaminidase activity in glycan chain length determination in *S. aureus*. Strains lacking *sagB* had substantially longer glycan strands than did SH1000. The presence or absence of other glucosaminidase-encoding genes (*atl*, *sagA*, and *scaH*) had minimal effect on strand length. Annotations show proportions of glycan strands within ranges of numbers of disaccharides (DS); grey traces show the proportions in SH1000 cells for comparison. To compensate for the fact that longer glycan strands incorporate more [^{14}C]GlcNAc, radioactivity counts (cpm) were divided by the corresponding theoretical molecular weight (see Materials and Methods). The glycan chain abundance is plotted normalized relative to the maximal ratio between radioactivity counts and theoretical molecular weight (cpm/MW).

ence of functional *atl*, *sagA*, and *scaH* did not compensate for *sagB* inactivation. The glycan chain length distributions of SH1367 (*atl*), SH4606 (*sagA*), and SH4607 (*scaH*) were similar to that of SH1000 (see Fig. S5 in the supplemental material). Given the dominant role of SagB in glycan chain length reduction, its activity likely masks any more subtle combined, mutually redundant role of the other three enzymes.

The capability of SagB to hydrolyze peptidoglycan was confirmed *in vitro* (using *B. subtilis* peptidoglycan as a substrate) by zymogram assay (see Fig. S7a in the supplemental material). There was more complete hydrolysis when the assay was carried out at pH 5 than at pH 7.5. *B. subtilis* peptidoglycan is a useful and appropriate substrate, as it has previously been shown to have long glycan strands compared to those of *S. aureus* (21). *B. subtilis* purified glycan chains were digested with recombinant SagB or Atl (glucosaminidase domain) and analyzed by size exclusion chromatography (see Fig. S7b). Both SagB- and Atl (glucosaminidase domain)-digested material had a lower molecular weight than undigested glycan strands. Material digested by Atl (glucosaminidase domain) had an overall lower molecular weight than that digested by SagB. This indicates a partial digestion by SagB compared to the digestion by Atl (glucosaminidase domain), suggesting a preferential activity by SagB on longer glycan strands as substrates (i.e., an inability to hydrolyze shorter strands).

SagB has a minimal role in cell separation. The effect of hydrolase inactivation on cell separation was investigated using flow cytometry and optical microscopy. Those strains lacking Atl exhibited higher levels of forward scatter than other strains (forward scatter tends to be higher for larger objects, i.e., larger clumps; see Fig. S8a in the supplemental material), a finding qualitatively confirmed by optical microscopy (see Fig. S8b), suggesting a less important role in this process for SagA, SagB, and ScaH. However, the highest level of forward scatter was observed for SH4611 (*atl sagA scaH*), demonstrating a combined effect.

DISCUSSION

The group of hydrolases we have studied here exhibit functional redundancy in terms of population growth, and only by inactivating *sagA*, *atl*, and *scaH* and depleting *sagB* expression do we see that it is critical for the bacteria to retain at least one of the products of these genes. We have also shown that it is only under conditions where glucosaminidase activity has been effectively removed that *S. aureus* cells are impaired in their ability to enlarge normally. It seems clear that this inability to enlarge at the cellular level explains the population growth defects.

In light of this redundancy, it is surprising to see that SagB is by far the dominant enzyme in terms of the effect on glycan chain length. *S. aureus* has short glycan chains relative to those of other Gram-positive bacteria for which size exclusion High-Performance Liquid Chromatography (HPLC) measurements have been made (20, 21, 27). Our data show that the processivity of enzymes that insert peptidoglycan into the sacculus by forming glycosidic bonds (PBP2, MGT, and SgtA [28]) is not responsible for the predominance of short glycan chains but, instead, that chains are subsequently processed by SagB. Inactivation of *sagB* alone is enough to increase cell surface stiffness, a phenomenon explicable simply in terms of the dependence of the bulk properties of a polymer on the number of cross-links between individual chains; this explanation is supported by the discovery that peptide cross-linking levels also affect stiffness (29). This establishes a clear relationship between glycan chain length and cell surface stiffness. However, inactivation of *sagA*, *atl*, and *scaH* together also led to an increase in stiffness, although not as great as that caused by inactivation of *sagB*. This is despite there being no apparent alteration from the wild-type chain length in SH4611 (*atl sagA scaH*). We interpret this as evidence that these hydrolases affect cell surface stiffness with minimal influence on the overall glycan chain length, most likely by breaking a small number of bonds, bonds in specific locations in the chains, or bonds in specific locations within the sacculus. Nevertheless, active *sagB* is unable to fully compensate for their absence. Ultimately, it seems that cellular enlargement depends on reduction of cell wall stiffness mediated by hydrolases, with a concomitant alteration to the peptidoglycan structure and architecture.

While there have been many proposals describing detailed mechanisms by which peptidoglycan is inserted into the cell wall during enlargement of bacterial cells, the overarching concept is that unstressed material is added before parts of the preexisting

TABLE 1 Strains used in this study

Species	Strain	Relevant genotype or description	Source
E. coli	BL21 (DE3)	F$^-$ *ompT hsdSB* (r_B^- m_B^-) *gal dcm* (DE3)	Novagen
	TOP10	F$^-$ *mcrA* Δ(*mrr-hsdRMS-mcrBC*) ϕ80 *lacZ* Δ*M15* Δ*lacX74 recA1deoR araD139* Δ(*ara-leu*)*7697 galK rpsL* Str^r *endA1 nupG*	Invitrogen
	SH3062	BL21(DE3) pET24d+ *sagB* overexpression construct	
	SH3061	*E. coli* BL21(DE3) pSRC002	36
	SH2195	*E. coli* BL21(DE3) pSRC003	36
S. aureus	SH1000	Functional *rsbU*$^+$ derivative of 8325-4	37
	SH1367 (*atl*)	SH1000 [*atl*::*pAZ106* (*ery lin*)]	23
	SH4091 (*atl*::*spc*)	SA113 (*atl*::*spc*)	38
	SH4606 (*sagA*)	SH1000 (*sagA*::*tet*)	This study
	SH4607 (*scaH*)	SH1000 [*scaH*::*tet*(M)]	This study
	SH4608 (*sagB*)	SH1000 (*sagB*::*kan*)	This study
	SH4609 [*sagB geh*(*sagB*$^+$)][a]	SH1000 (*sagB*::*kan geh*::*sagB*)	This study
	SH4610 (*atl sagA sagB*)	SH1000 (*atl*::*pAZ106 sagA*::*tet sagB*::*kan*)	This study
	SH4611 (*atl sagA scaH*)	SH1000 [*atl*::*spc sagA*::*tet scaH*::*tet*(M)]	39; this study
	SH4612 (*sagA sagB scaH*)	SH1000 [*sagA*::*tet sagB*::*kan scaH*::*tet*(M)]	This study
	SH4613 (*atl sagB scaH*)	SH1000 [*atl*::*pAZ106 sagB*::*kan scaH*::*tet*(M)]	This study
	SH4614 (P_{spac}-*sagB*)	SH1000 (P_{spac}-*sagB*)	This study
	SH4615 (P_{spac}-*sagB atl sagA scaH*)	SH1000 [P_{spac}-*sagB atl*::*spc sagA*::*tet scaH*::*tet*(M)]	This study
	SH4090	RN4220 (P_{spac}-*sagB* Ery^r)	This study
	RN4220	Restriction-deficient derivative of 8325-4	40
	RN6911	*agr*::*tet*(M) derivative of RN6390	41
B. subtilis	168 HR	Wild type	Howard Rogers

[a] Chromosomal *sagB* complementation construct abbreviated to *geh*(*sagB*$^+$) in the main text.

sacculus are hydrolyzed to enable expansion. We have shown a mechanistic basis for this in *S. aureus*, where hydrolysis of peptidoglycan modulates the mechanical properties of the cell wall, which enables irreversible expansion of the cell. A unifying model across the bacteria can be invoked in which dense, stiff regions of peptidoglycan are initially formed, becoming less dense and less stiff as they are hydrolyzed and, thus, enabling enlargement of the cell surface area; this model is independent of the detailed mechanism of monomer insertion and mode of hydrolysis. In *E. coli*, the insertion of new peptidoglycan is targeted to less dense, more porous regions of the cell wall (1, 30) via an established mechanism involving inner and outer membrane proteins (31, 32), mak-

TABLE 2 Plasmids used in this study

Plasmid	Relevant background/genotype/markers	Source
pAZ106	Promoterless transcriptional *lacZ* fusion vector, used as a *lacZ* expression reporter plasmid; Amp^r (*E. coli*), Ery^r (*S. aureus*)	42
pDG1513	Vector carrying *tet* cassette suitable for selection in Gram-positive bacteria; Min^r Tet^r	43
pET24d	His_6 tag overexpression vector; Kan^r	Novagen
pET24d-SagB	pET24d containing the *sagB* sequence, minus the signal sequence, upstream from the His_6 tag	
pGL433b	Vector carrying *kan* cassette suitable for selection in Gram-positive bacteria; Kan^r	J. Garcia-Lara and S. J. Foster, unpublished data
pInvSA	pUC19 containing a 2.4-kb fragment of the region spanning the *sagB* gene in which the *sagB* gene has been inactivated by a 600-bp deletion; Amp^r	
pMUTIN4	Insertion vector carrying IPTG-inducible P_{spac} promoter; Amp^r (*E. coli*), Ery^r (*S. aureus*)	44
pRW01	pMUTIN4 insertion vector carrying P_{spac} promoter and 650-bp fragment of *sagB*; Amp^r (*E. coli*), Ery^r (*S. aureus*)	
pSA18Kan	pMUTIN4 containing EcoRI-BamHI-cut fragment of pInvSA and 1.5 kb Kan^r cassette from pGL433 within disrupted *sagB* construct at KpnI restriction site; Amp^r (*E. coli*), Ery^r (*S. aureus*), Kan^r	
pSA26Min2	pSA26D with *tet*(M) cassette of *S. aureus* RN6911 inserted into KpnI site within the *scaH* gene; Amp^r (*E. coli*), Ery^r (*S. aureus*), *tet*(M) resistance gene	
pSA26D	pMUTIN4 containing 2.7-kb fragment of *scaH* and ~1 kb of flanking region; Amp^r (*E. coli*), Ery^r (*S. aureus*)	
pSRC002	*atl* amidase domain overexpression construct	36
pSRC003	*atl* glucosaminidase domain overexpression construct	36
pKASBAR	pUC18 vector containing *attP* and *tet* cassette (Amp^r Tet^r)	45
pKASBAR-sagB	pKASBAR containing a 1,357-bp fragment, including the *sagB* gene and promoter region, inserted between EcoRI and BamHI restriction sites; pUC19 *E. coli* cloning vector (Amp^r)	NEB
pCR 2.1-TOPO	TOPO TA cloning vector; Amp^r Kan^r	Life Technologies

[a] Amp^r, ampicillin resistance; Ery^r, erythromycin resistance; Kan^r, kanamycin resistance; Tet^r, tetracycline resistance; Min^r, minocycline resistance.

TABLE 3 Oligonucleotides used in this study

Primer	Sequence (5′–3′)[a]	Restriction site
RW01_F	TTTTTT**GAATTC**AACAATGACCTAAGAGGTGTGGA	EcoRI
RW01_R	TTTTTT**GGATCC**CAACCATGCTTTTTAGC	BamHI
P1	CGGGC**TCTAGA**TAATCCACACAGCTGGCGTCTTAGC	XbaI
P2	CGGCC**GGTACC**AGGATCTGTTTCGAATAATGATGTTGC	KpnI
FD2	CGGCG**GGTACC**AACATCATTATTCGAAACAGATCCTAG	KpnI
RD2	CGGGC**AAGCTT**TATTTACGTGCAAATGATATTAATC	HindIII
FKan	GGCGG**GGTACC**CAGCGAACCATTTGAGG	KpnI
RKan	GGGGC**GGTACC**AATTCCTCGTAGGCGCTCGG	KpnI
P6	GGGCC**GGATCC**TTCAAGGTATAGTTTGAGCC	BamHI
P7	TATTAT**GAGCTC**TATCGTCGTATTCGGCTTAAG	SacI
MinFK3	AACAA**GGTACC**AATATGCTCTTACGTGCT	KpnI
MinRK4	AACAA**GGTACC**AGAAATATTGAAGCTAGT	KpnI
InvF1	GCGCGG**GGTACC**AGAACATGAAGACTGAAGGAA	KpnI
InvR1	GCGCGG**GGTACC**TTCAATCTTAATGTCGGAT	KpnI
SagA-F1	CGAC**GGATCC**TAACGGAACAATACCTACTC	BamHI
SagA-R1	ATAACT**GCGGCCGC**GAGTGACATTCGCTGGGCAG	NotI
SagA-F2	CC**GGTACC**TTCACGATGAGTAATACAGC	KpnI
SagA-R2	ACAT**GAATTC**AACCGCAGTACAGTGTTC	EcoRI
Tet-NotI	ATAACT**GCGGCCGC**GGATTTTATGACCGATGATGAAG	NotI
Tet-KpnI	CC**GGTACC**TGTTATAAAAAAAGGATCAAT	KpnI
rSagB_For	GCGC**CCATGG**TATCCGATCAGATATTTTTCAAACATGTT	NcoI
rSagB_Rev	GCGC**CTCGAG**CTTATTCAAATGTTTACTGTCATC	XhoI
1825C_For	TTTTTT**GAATTC**GGTCAAATTGAAGGCACGAT	EcoRI
1825C_Rev	TTTTTT**GGATCC**TTGCATTGGTGGGATTATCA	BamHI
Geh_For	GAGGTGCTGACAATGATGAAAA	
Geh_Rev	CCGATTAATTGAAAGAAGTCTGC	

[a] Restriction sites included for cloning purposes are indicated in bold font.

ing these regions more dense. Hydrolysis and expansion of these regions would allow for enlargement. In *B. subtilis*, the detailed mechanism of peptidoglycan insertion is less well understood (27, 33), but essential hydrolase activity is required for cell enlargement (6). All of the proposed growth modes are compatible with the general principle of reduction in peptidoglycan density and increase in elasticity through hydrolase activity to enable enlargement, as demonstrated here for *S. aureus*.

MATERIALS AND METHODS

Bacterial strains, plasmids, and primers. The *S. aureus* strains used in this study are listed in Table 1, plasmids are listed in Table 2, and primers in Table 3.

Growth conditions and media. All *S. aureus* strains were grown in brain heart infusion (BHI) broth at 37°C with aeration at 250 rpm unless otherwise stated. *E. coli* and *B. subtilis* strains were routinely grown in Luria-Bertani (LB) medium or Nutrient Broth, respectively, at 37°C with aeration at 250 rpm. For solid media, 1.5% (wt/vol) agar was added. Where required, selection for antibiotic resistance markers was carried out using the following concentrations of drugs: Amp^r, ampicillin (100 μg/ml); Chl^r, chloramphenicol (30 μg/ml); Ery^r, erythromycin (5 μg/ml) with lincomycin (25 μg/ml); Kan^r, kanamycin (50 μg/ml) with neomycin (50 μg/ml); Min^r, minocycline (2 μg/ml); Spc^r, spectinomycin (100 μg/ml); Tet^r, tetracycline (5 μg/ml).

Genetic modification of bacteria. Transformation by electroporation of *E. coli* or the restriction-deficient *S. aureus* RN4220 strain was performed according to published methods (34, 35). Phage transduction into the *S. aureus* SH1000 background using φ11 or φ85 was carried out as described previously (23). Details of construction of strains can be found in Text S1 in the supplemental material.

Overexpression and purification of recombinant enzymes. An overnight culture was used to inoculate 1 liter of preheated LB containing appropriate antibiotics for maintenance of the overexpression plasmid to an OD_{600} of 0.05. At an OD_{600} of approximately 0.4, 1 mM IPTG was added, and the culture incubated for a further 4 h. Cells were harvested by centrifugation and stored as pellets at −80°C. Pellets were freeze-thawed three times in sodium phosphate buffer and sonicated on ice six times. Insoluble material was separated by centrifugation at 10,000 × *g* for 30 min. The supernatant was filter sterilized (0.45-μm filters) and purified using a 5-ml HiTrap column (Amersham) with a BioRad Econo gradient pump and fraction collector. The His-tagged proteins were eluted from the column using an isocratic gradient of 5-to-60% 0.5 M imidazole over 30 min. Eluted fractions were analyzed by SDS-PAGE. Fractions containing overexpressed protein were pooled, transferred to dialysis tubing, and dialyzed three times in phosphate-buffered saline (PBS) for 18 h in total. The identities of purified, overexpressed proteins were confirmed by N-terminal sequencing.

Analysis of autolysin activity by zymograms. The lytic activity of the recombinant glucosaminidases was investigated by zymogram (23), using purified cell walls of vegetative *B. subtilis* as a substrate.

Purification of sacculi. Bacterial cultures were grown to exponential phase (OD_{600} of ~0.5), and peptidoglycan purified as described previously (11). Briefly, cells were broken by mechanical shearing using a FastPrep homogenizer (*S. aureus*) or French press (*B. subtilis*). Sacculi were extracted by boiling in SDS (4% wt/vol), Pronase (2 mg/ml) treatment, and removal of accessory polymers by incubation in hydrofluoric acid (48% vol/vol) at 4°C for 48 h. Purified sacculi were washed extensively (at least six times) in water after SDS or hydrofluoric acid treatment. Long-term storage of sacculi was at −20°C. Radiolabeling with *N*-acetyl[^{14}C]glucosamine ([^{14}C]GlcNAc) was carried out as described previously (21). Briefly, exponential-phase (OD_{600} of 0.3) cultures were diluted in 50 ml of prewarmed LB containing 0.185 MBq [^{14}C]GlcNAc (1.67 TBq/mmol; Hartmann Analytic) and 500 ml of nonradioactive medium to give a starting OD_{600} of 0.04. After three generations, the cells were harvested by centrifugation and sacculi purified.

Purification of glycan strands. Glycan strands were purified as previously described (21). Radiolabeled peptidoglycan sacculi were digested by recombinant *S. aureus* Atl amidase domain (36). Typically, 1 mg of pep-

tidoglycan was digested overnight with Atl at a concentration 5-fold greater than that required to solubilize more than 90% of the peptidoglycan. The enzyme was inactivated by boiling (3 min), and the supernatants were collected for further analysis.

Plating efficiency of conditional mutant. A single colony of SH4615 (P_{spac}-*sagB atl sagA scaH*) was taken from an agar plate containing 1 mM IPTG and appropriate antibiotics using a sterile inoculation loop and was resuspended in 10 ml PBS. A cotton bud was then used to streak this suspension onto plates containing 1 mM IPTG or lacking IPTG.

Liquid growth of conditional mutant. Colonies were taken from agar plates containing appropriate antibiotics [and 1 mM IPTG in the case of SH4615 (P_{spac}-*sagB atl sagA scaH*)] using a sterile inoculation loop. These were individually resuspended in 1 ml BHI. Subsequently, these suspensions were used to inoculate 50 ml BHI in 250-ml conical flasks to a calculated OD_{600} of 0.001, and the flasks were incubated at 37°C with agitation at 250 rpm, with optical density measurements taken periodically. Strains were sonicated prior to measurements of optical density and inoculations to reduce the potential effects of clumping.

Time-lapse microscopy. Bacteria were grown overnight at 37°C with agitation at 250 rpm in BHI and then subcultured to an OD_{600} of ~0.05 and grown under the same conditions to an OD_{600} of ~0.3. Subsequently, 2 μl of this culture was pipetted onto an agarose pad containing 0.5 μg/ml FM 1-43 (Molecular Probes), allowed to partially dry, and then topped with a coverslip before being imaged using a Nikon Eclipse inverted epifluorescence microscope equipped with an incubator used to hold the experiment at 37°C.

Imaging cells labeled with fluorescent vancomycin or WGA. BHI medium was used throughout. Strains were sonicated prior to measurements of optical density and inoculations to reduce the potential effects of clumping. Strains were grown overnight in the presence of appropriate antibiotics and, in the case of SH4615 (P_{spac}-*sagB atl sagA scaH*), 1 mM IPTG. Starter cultures [containing no antibiotics but with 10 μM IPTG in the case of SH4615 (P_{spac}-*sagB atl sagA scaH*)] were then inoculated. These were incubated at 37°C with agitation at 250 rpm until they reached an OD_{600} of ~1. A 10-ml sample was then washed once in prewarmed BHI and used to inoculate cultures from which microscopy samples would be taken. One millimolar IPTG was added to one culture of SH4615 (P_{spac}-*sagB atl sagA scaH*) to induce the expression of *sagB*, while another was left without IPTG. Samples for microscopy were taken from exponential-phase cultures and then labeled with Van-FL and imaged as previously described (11). Fluorescent WGA (Molecular Probes) labeling took place after Van-FL labeling but before fixing cells. Cells were resuspended in 250 μl distilled water containing 1 mM $CaCl_2$ and 100 μg/ml fluorescent WGA and then washed three times by centrifugation.

Cell wall stiffness measurements. Cell wall stiffness measurements were carried out as described previously (16). Briefly, samples of cells of each strain to be studied were grown to exponential phase and then washed and immobilized on a microstructure (24). Bacteria were indented repeatedly under BHI medium, a curve from an equivalent indentation on an incompressible material subtracted, and the tangent to the resulting force versus indentation curves used to derive a relative effective spring constant to obtain a measure of stiffness.

HPLC separation of glycan strands. Size exclusion chromatography of glycan strands was performed as described previously (21, 27). Approximately 20,000 cpm of each radiolabeled glycan strand fraction (corresponding to 50 to 100 μg peptidoglycan) was injected in a volume of 200 μl onto a TSKSW2000 (7.5 by 600 mm) size exclusion HPLC column (Tosoh) preequilibrated in 100-mM phosphate buffer (pH 6.0). Elution was carried out at a flow rate of 0.4 ml/min. Radiolabeled glycan strands were detected with a LabLogic (β-Ram model 4) radio flow detector using a 1:1 scintillation cocktail and a 100-μl solid cell. The gel filtration columns were calibrated as described previously (21), using dextran standards ranging from 1 kDa to 150 kDa (analytical standard grade for GPC; Sigma-Aldrich). Analysis of the glycan strand distribution was carried out as described previously (21).

Flow cytometry analysis Bacteria were incubated overnight with agitation at 37°C. Ten milliliters of fresh BHI was inoculated with 100 μl of overnight culture (dilution of 1:100). Bacteria were incubated to an OD_{600} of 0.3 to 0.4 (early exponential phase) and then diluted 1:100 in PBS. The samples were analyzed by flow cytometry using an Attun autosampler and imaged using a Novex optical microscope.

SUPPLEMENTAL MATERIAL

Supplemental material for this article may be found at http://mbio.asm.org/lookup/suppl/doi:10.1128/mBio.00660-15/-/DCSupplemental.

Figure S1, PDF file, 0.5 MB.
Figure S2, PDF file, 0.2 MB.
Figure S3, PDF file, 0.3 MB.
Figure S4, PDF file, 0.4 MB.
Figure S5, PDF file, 0.3 MB.
Figure S6, PDF file, 0.3 MB.
Figure S7, PDF file, 0.2 MB.
Figure S8, PDF file, 0.3 MB.
Table S1, PDF file, 0.2 MB.
Text S1, PDF file, 0.4 MB.

ACKNOWLEDGMENTS

This work was funded by Biotechnology and Biological Sciences Research Council (BBSRC grants BB/H011005/1 and BBL006162/1) and made use of facilities provided through the Medical Research Council (MRC)-funded SHIMA project (grant MR/K015753/1). S.M. was supported by a Marie Curie intra-European Fellowship (251336). The Royal Society funded equipment.

REFERENCES

1. **Typas A, Banzhaf M, Gross CA, Vollmer W.** 2012. From the regulation of peptidoglycan synthesis to bacterial growth and morphology. Nat Rev Microbiol **10:**123–136. http://dx.doi.org/10.1038/nrmicro2677.
2. **Koch AL, Doyle RJ.** 1985. Inside-to-outside growth and turnover of the wall of gram-positive rods. J Theor Biol **117:**137–157. http://dx.doi.org/10.1016/S0022-5193(85)80169-7.
3. **Höltje J-V.** 1993. Three for one —a simple growth mechanism that guarantees a precise copy of the thin, rod-shaped murein sacculus of *Escherichia coli*, p 419–426. In de Pedro MA, Höltje J-V, Löffelhardt W (ed), Bacterial growth and lysis: metabolism and structure of the bacterial sacculus. Springer, New York, NY.
4. **Bartual SG, Straume D, Stamsås GA, Muñoz IG, Alfonso C, Martínez-Ripoll M, Håvarstein LS, Hermoso JA.** 2014. Structural basis of PcsB-mediated cell separation in *Streptococcus pneumoniae*. Nat Commun **5:**3842. http://dx.doi.org/10.1038/ncomms4842.
5. **Sham L-T, Barendt SM, Kopecky KE, Winkler ME.** 2011. Essential PcsB-putative peptidoglycan hydrolase interacts with the essential $FtsX_{Spn}$ cell division protein in *Streptococcus pneumoniae* D39. Proc Natl Acad Sci U S A **108:**E1061–E1069. http://dx.doi.org/10.1073/pnas.1108323108.
6. **Bisicchia P, Noone D, Lioliou E, Howell A, Quigley S, Jensen T, Jarmer H, Devine KM.** 2007. The essential YycFG two-component system controls cell wall metabolism in *Bacillus subtilis*. Mol Microbiol **65:**180–200. http://dx.doi.org/10.1111/j.1365-2958.2007.05782.x.
7. **Singh S, SaiSree, Amrutha R, Reddy M.** 2012. Three redundant murein endopeptidases catalyze an essential cleavage step in peptidoglycan synthesis of *Escherichia coli* K12. Mol Microbiol. **86:**1036–1051. http://dx.doi.org/10.1111/mmi.12058.
8. **Vollmer W.** 2012. Bacterial growth does require peptidoglycan hydrolases. Mol Microbiol **86:**1031–1035. http://dx.doi.org/10.1111/mmi.12059.
9. **Pinho MG, Kjos M, Veening J-W.** 2013. How to get (a)round: mechanisms controlling growth and division of coccoid bacteria. Nat Rev Microbiol **11:**601–614. http://dx.doi.org/10.1038/nrmicro3088.
10. **Uehara T, Bernhardt TG.** 2011. More than just lysins: peptidoglycan hydrolases tailor the cell wall. Curr Opin Microbiol **14:**698–703. http://dx.doi.org/10.1016/j.mib.2011.10.003.
11. **Turner R, Ratcliffe E, Wheeler R, Golestanian R, Hobbs J, Foster S.** 2010. Peptidoglycan architecture can specify division planes in *Staphylococcus aureus*. Nat Commun **1:**1–9.
12. **Pinho MG, Errington J.** 2005. Recruitment of penicillin-binding protein

PBP2 to the division site of *Staphylococcus aureus* is dependent on its transpeptidation substrates. Mol Microbiol **55:**799–807. http://dx.doi.org/10.1111/j.1365-2958.2004.04420.x.

13. **Zhou X, Halladin DK, Rojas ER, Koslover EF, Lee TK, Huang KC, Theriot JA.** 2015. Mechanical crack propagation drives millisecond daughter cell separation in *Staphylococcus aureus*. Science **348:**574–578. http://dx.doi.org/10.1126/science.aaa1511.
14. **Tzagoloff H, Novick R.** 1977. Geometry of cell division in *Staphylococcus aureus*. J Bacteriol **129:**343–350.
15. **Touhami A, Jericho MH, Beveridge TJ.** 2004. Atomic force microscopy of cell growth and division in *Staphylococcus aureus*. J Bacteriol **186:** 3286–3295. http://dx.doi.org/10.1128/JB.186.11.3286-3295.2004.
16. **Bailey RG, Turner RD, Mullin N, Clarke N, Foster SJ, Hobbs JK.** 2014. The interplay between cell wall mechanical properties and the cell cycle in *Staphylococcus aureus*. Biophys J **107:**2538–2545. http://dx.doi.org/10.1016/j.bpj.2014.10.036.
17. **Frankel MB, Hendrickx AP, Missiakas DM, Schneewind O.** 2011. LytN, a murein hydrolase in the cross-wall compartment of *Staphylococcus aureus*, is involved in proper bacterial growth and envelope assembly. J Biol Chem **286:**32593–32605. http://dx.doi.org/10.1074/jbc.M111.258863.
18. **Frankel MB, Schneewind O.** 2012. Determinants of murein hydrolase targeting to cross-wall of *Staphylococcus aureus* peptidoglycan. J Biol Chem **287:**10460–10471. http://dx.doi.org/10.1074/jbc.M111.336404.
19. **Stapleton MR, Horsburgh MJ, Hayhurst EJ, Wright L, Jonsson I-M, Tarkowski A, Kokai-Kun JF, Mond JJ, Foster SJ.** 2007. Characterization of IsaA and SceD, two putative lytic transglycosylases of *Staphylococcus aureus*. J Bacteriol **189:**7316–7325. http://dx.doi.org/10.1128/JB.00734-07.
20. **Boneca IG, Huang Z-H, Gage DA, Tomasz A.** 2000. Characterization of *Staphylococcus aureus* cell wall glycan strands, evidence for a new β-*N*-acetylglucosaminidase activity. J Biol Chem **275:**9910–9918. http://dx.doi.org/10.1074/jbc.275.14.9910.
21. **Wheeler R, Mesnage S, Boneca IG, Hobbs JK, Foster SJ.** 2011. Super-resolution microscopy reveals cell wall dynamics and peptidoglycan architecture in ovococcal bacteria. Mol Microbiol **82:**1096–1109. http://dx.doi.org/10.1111/j.1365-2958.2011.07871.x.
22. **Oshida T, Sugai M, Komatsuzawa H, Hong YM, Suginaka H, Tomasz A.** 1995. A *Staphylococcus aureus* autolysin that has an *N*-acetylmuramoyl-L-alanine amidase domain and an endo-β-*N*-acetylglucosaminidase domain: cloning, sequence analysis, and characterization. Proc Natl Acad Sci U S A **92:**285–289. http://dx.doi.org/10.1073/pnas.92.1.285.
23. **Foster SJ.** 1995. Molecular characterization and functional analysis of the major autolysin of *Staphylococcus aureus* 8325/4. J Bacteriol **177:** 5723–5725.
24. **Kailas L, Ratcliffe EC, Hayhurst EJ, Walker MG, Foster SJ, Hobbs JK.** 2009. Immobilizing live bacteria for AFM imaging of cellular processes. Ultramicroscopy **109:**775–780. http://dx.doi.org/10.1016/j.ultramic.2009.01.012.
25. **Turner RD, Thomson NH, Kirkham J, Devine D.** 2010. Improvement of the pore trapping method to immobilize vital coccoid bacteria for high-resolution AFM: a study of *Staphylococcus aureus*. J Microsc **238:**102–110. http://dx.doi.org/10.1111/j.1365-2818.2009.03333.x.
26. **Daniel RA, Errington J.** 2003. Control of cell morphogenesis in bacteria: two distinct ways to make a rod-shaped cell. Cell **113:**767–776. http://dx.doi.org/10.1016/S0092-8674(03)00421-5.
27. **Hayhurst EJ, Kailas L, Hobbs JK, Foster SJ.** 2008. Cell wall peptidoglycan architecture in *Bacillus subtilis*. Proc Natl Acad Sci U S A **105:** 14603–14608. http://dx.doi.org/10.1073/pnas.0804138105.
28. **Reed P, Veiga H, Jorge AM, Terrak M, Pinho MG.** 2011. Monofunctional transglycosylases are not essential for *Staphylococcus aureus* cell wall synthesis. J Bacteriol **193:**2549–2556. http://dx.doi.org/10.1128/JB.01474-10.
29. **Loskill P, Pereira PM, Jung P, Bischoff M, Herrmann M, Pinho MG, Jacobs K.** 2014. Reduction of the peptidoglycan crosslinking causes a decrease in stiffness of the *Staphylococcus aureus* cell envelope. Biophys J **107:**1082–1089. http://dx.doi.org/10.1016/j.bpj.2014.07.029.
30. **Turner R, Hurd A, Cadby A, Hobbs J, Foster S.** 2013. Cell wall elongation mode in gram-negative bacteria is determined by peptidoglycan architecture. Nat Commun **4:**1496. http://dx.doi.org/10.1038/ncomms2503.
31. **Typas A, Banzhaf M, van den Berg van Saparoea B, Verheul J, Biboy J, Nichols RJ, Zietek M, Beilharz K, Kannenberg K, von Rechenberg M, Breukink E, den Blaauwen T, Gross CA, Vollmer W.** 2010. Regulation of peptidoglycan synthesis by outer-membrane proteins. Cell **143:** 1097–1109. http://dx.doi.org/10.1016/j.cell.2010.11.038.
32. **Paradis-Bleau C, Markovski M, Uehara T, Lupoli TJ, Walker S, Kahne DE, Bernhardt TG.** 2010. Lipoprotein cofactors located in the outer membrane activate bacterial cell wall polymerases. Cell **143:**1110–1120. http://dx.doi.org/10.1016/j.cell.2010.11.037.
33. **Beeby M, Gumbart JC, Roux B, Jensen GJ.** 2013. Architecture and assembly of the Gram-positive cell wall. Mol Microbiol **88:**664–672. http://dx.doi.org/10.1111/mmi.12203.
34. **Sambrook J, Russell D.** 2001. Molecular cloning: a laboratory manual. Cold Spring Harbor Laboratory Press, New York, NY.
35. **Schenk S, Laddaga RA.** 1992. Improved method for electroporation of *Staphylococcus aureus*. FEMS Microbiol Lett **73:**133–138.
36. **Clarke SR, Brummell KJ, Horsburgh MJ, McDowell PW, Mohamad SA, Stapleton MR, Acevedo J, Read RC, Day NP, Peacock SJ, Mond JJ, Kokai-Kun JF, Foster SJ.** 2006. Identification of in vivo-expressed antigens of *Staphylococcus aureus* and their use in vaccinations for protection against nasal carriage. J Infect Dis **193:**1098–1108. http://dx.doi.org/10.1086/501471.
37. **Horsburgh MJ, Aish JL, White IJ, Shaw L, Lithgow JK, Foster SJ.** 2002. σ^B modulates virulence determinant expression and stress resistance: characterization of a functional rsbU strain derived from *Staphylococcus aureus* 8325-4. J Bacteriol **184:**5457–5467. http://dx.doi.org/10.1128/JB.184.19.5457-5467.2002.
38. **Pasztor L, Ziebandt A-K, Nega M, Schlag M, Haase S, Franz-Wachtel M, Madlung J, Nordheim A, Heinrichs DE, Götz F.** 2010. Staphylococcal major autolysin (Atl) is involved in excretion of cytoplasmic proteins. J Biol Chem **285:**36794–36803. http://dx.doi.org/10.1074/jbc.M110.167312.
39. **Mohamad SAS.** 2007. Ph.D. thesis. University of Sheffield, Sheffield, South Yorkshire, United Kingdom.
40. **Kreiswirth BN, Löfdahl S, Betley MJ, O'Reilly M, Schlievert PM, Bergdoll MS, Novick RP.** 1983. The toxic shock syndrome exotoxin structural gene is not detectably transmitted by a prophage. Nature **305:**709–712. http://dx.doi.org/10.1038/305709a0.
41. **Novick RP, Ross HF, Projan SJ, Kornblum J, Kreiswirth B, Moghazeh S.** 1993. Synthesis of staphylococcal virulence factors is controlled by a regulatory RNA molecule. EMBO J **12:**3967–3975.
42. **Kemp EH, Sammons RL, Moir A, Sun D, Setlow P.** 1991. Analysis of transcriptional control of the *gerD* spore germination gene of *Bacillus subtilis* 168. J Bacteriol **173:**4646–4652.
43. **Guérout-Fleury AM, Shazand K, Frandsen N, Stragier P.** 1995. Antibiotic-resistance cassettes for *Bacillus subtilis*. Gene **167:**335–336. http://dx.doi.org/10.1016/0378-1119(95)00652-4.
44. **Vagner V, Dervyn E, Ehrlich SD.** 1998. A vector for systematic gene inactivation in *Bacillus subtilis*. Microbiology **144:**3097–3104. http://dx.doi.org/10.1099/00221287-144-11-3097.
45. **Bottomley AL, Kabli AF, Hurd AF, Turner RD, Garcia-Lara J, Foster SJ.** 2014. *Staphylococcus aureus* DivIB is a peptidoglycan-binding protein that is required for a morphological checkpoint in cell division. Mol Microbiol **94:**1041–1064. http://dx.doi.org/10.1111/mmi.12813.